

Microstructural Characterization and Consolidation of Severely Deformed Copper Powder Reinforced with Multiwalled Carbon Nanotubes

M.R. AKBARPOUR^{a,*} AND E. SALAHI^b

^aDepartment of Materials Engineering, Faculty of Engineering, University of Maragheh, Maragheh, East Azerbaijan, Iran

^bMaterials and Energy Research Center (MERC), P.O. Box 14155-4777, Tehran, Iran

(Received October 31, 2014)

In this paper, the mechanical milling process for various durations was used to generate a homogeneous distribution of 1 wt.% carbon nanotube within Cu powder. Effects of milling time on morphology, microstructure, and microhardness of the powder were studied. The results showed that work hardened Cu-carbon nanotube nanocomposite powder with nanosized grains can be fabricated by the mechanical milling of the elemental materials. The addition of carbon nanotubes accelerated the morphological and microstructural evolution during the mechanical milling and influenced the compressibility of the powder. The compressibility behavior of the powder was analyzed using analytical models and used to estimate the strength of the powder. The nanocomposite compacts were sintered in vacuum and showed the maximum relative density of $\approx 91\%$ at optimum condition.

DOI: [10.12693/APhysPolA.127.1722](https://doi.org/10.12693/APhysPolA.127.1722)

PACS: 81.05.Ni, 88.30.rh, 81.07.Bc, 64.70.fm

1. Introduction

Carbon nanotubes (CNTs) have attracted scientific and technological interest because of their significant advantages in comparison with most existing materials. Many researchers have shown that carbon nanotubes possess remarkable mechanical properties, such as exceptionally high elastic modulus and high tensile strength [1–3]. There is growing interest in the addition of carbon nanotubes to metal matrixes, and large number of studies has been published to date. Researches show that the addition of carbon nanotubes can considerably enhance the strength, toughness and conductivities of metals [4–8]. There are some difficulties in using CNTs in metals which may result inferior mechanical properties of CNT/metal nanocomposites, which are severe agglomeration of CNTs, weak CNT/metal interface, and low relative density of CNT [9]. Various techniques have been used to solve these problems in CNT reinforced metals; for example: mechanical milling assisted hot/cold condensation, molecular level mixing, thermal spraying, deformation-based consolidation, co-deposition and so on [10]. Among metal–CNT composites, Cu–CNT composites are of interest because of superior mechanical and thermal properties of the fabricated composites. Therefore, many researches have been performed to fabricate this composite and enhance its properties by modifying the parameters influencing the composite characteristics.

Mechanical milling (MM) is one of the methods which are used to manufacture homogeneously dispersed CNT strengthened copper alloys. In the mechanical milling

process, repeated welding and fracturing of the powders by the impact energy between balls and the walls of the jar lead to homogeneous dispersion of CNTs and grain size refinement of the copper matrix. Mechanical milling of Cu–CNT and effect of the process parameters on CNT dispersion, powders morphology and microstructure have been studied by many researchers [11–14]. B.J. Kim et al. have synthesized Cu–CNT nanocomposite powder by ball milling followed by powder metallurgy processing. They have shown that the homogeneous Cu–CNT nanocomposite intermetallic particles with fine grains can be fabricated via this method [11]. T. Kim et al. [12] have studied the microstructure and tensile behavior of carbon nanotube reinforced Cu matrix nanocomposites fabricated by spark plasma sintering (SPS) of high energy ball-milled nanosized Cu powders reinforced with multi-wall CNTs followed by cold rolling process. Their results show that the mechanical milling can be used to prepare completely/partially homogeneous Cu/CNT powder for production of high strength bulk composites. In a recent work, Yoo et al. [14] have synthesized a high strength Cu–CNT nanocomposite by a combination of ball milling and high-ratio differential speed rolling. In their work, homogeneous dispersion of CNTs in nanostructured copper matrix was obtained by mechanical milling.

The literature data show that mechanical milling can be used as a method to obtain a homogeneous fine grained Cu–CNT composite powder which can be finally consolidated by many conventional techniques. The microstructure, morphology and hardness of Cu–CNT powder change during the mechanical milling process and can affect the microstructure, densification and mechanical features of consolidated final materials. Therefore, it is important to investigate these changes during the mechanical milling process and their effects on densification

*corresponding author; e-mail: mreza.akbarpour@gmail.com

behavior of the powder. Mechanical milling of Cu–CNT powder has been investigated by Shukla et al. [13]. They have shown the formation of layered structure by ball milling up to 20 h. They have studied the effect of mechanical milling time and CNT content on morphological changes and particle size during mechanical milling. The compressibility of the powders is a function of particle's size, hardness and morphology which are changing during mechanical milling. Since the green density of the powder is an important factor to obtain high density bulk materials after final cold/hot consolidation processes, hence, studying the effect of mechanical milling process on densification behavior of Cu–CNT powder is most important.

In the present study, mechanical milling of Cu–CNT powder in a planetary mill was carried out at various durations. Effect of mechanical milling on microstructure, morphology, and hardness of the powder were studied. The compressibility of the powders, mechanically milled for different times, was examined by uniaxial cold pressing. Three analytical models were used to estimate the green density of the powders compressed at different pressures and compared with experimental results. Finally, the mechanically milled powders for various times were vacuum sintered at different temperatures, and densification behavior was investigated.

2. Experimental procedure

Cu powder (Supplied from Merck corporation with 99.7% purity and particle size of $<60\ \mu\text{m}$) and multi-wall carbon nanotubes (MW-CNT) (approximately 20–30 nm in diameter and 3–4 μm in length) were used as starting materials. Transmission electron microscope image and X-ray diffraction pattern of the used CNT are shown in Fig. 1. 1 wt.% MWCNTs with Cu powder were

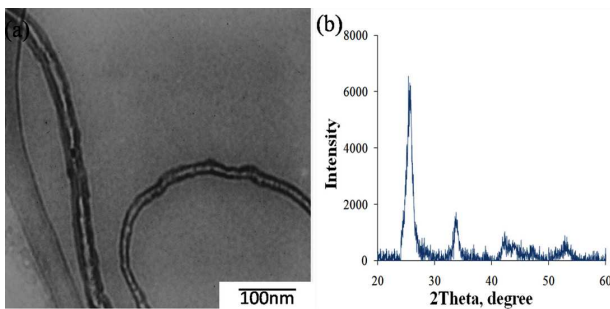


Fig. 1. (a) TEM micrograph and (b) XRD pattern of the used CNT.

placed in stainless steel mixing jars containing stainless steel milling balls of 10 and 15 mm diameter (giving an initial ball-to-powder weight ratio (BPR) = 10:1). The jars were filled with argon and were then agitated using a planetary ball mill at 300 rpm for milling time of 36 h. Samples were extracted from the batch after different mechanical milling times and investigated. The powders were analyzed by scanning electron microscope (Philips XL30), transmission electron microscope

and X-ray diffractometer (Philips (PW3710), Japan) to characterize the powders morphology and microstructure. X-ray diffraction analysis was performed using Cu K_{α} radiation ($\lambda = 1.54056\ \text{\AA}$). The mechanically milled powders for 0, 1, 8, 16, 24 and 36 h were each compressed at 300, 600, 800, and 1200 MPa, respectively, with zinc stearate as the die lubricant. The density of compact was measured by Archimedes' method. Three samples were examined at each pressure level to guarantee the accuracy of relative density, and the mean value of relative density obtained.

Finally, the mechanically milled powders were compressed at 1200 MPa and then sintered in a vacuum furnace ($<0.01\ \text{mbar}$) at different temperatures for 1 h. Densification of the sintered samples was evaluated by density measurement.

3. Results and discussion

3.1. Morphology

It is known that clustering is a major problem when the copper particles and CNTs are mixed, as a result of the large difference between densities of the both materials. Mechanical milling of the powders was used to solve the clustering problem and reach to homogeneous dispersion of CNTs. Figure 2 shows SEM micrographs of mechanically milled powder at various times illustrating the morphological changes of the powder during the mechanical milling process and qualitatively the dispersion of CNTs on the powders surface at initial times of mechanical milling.

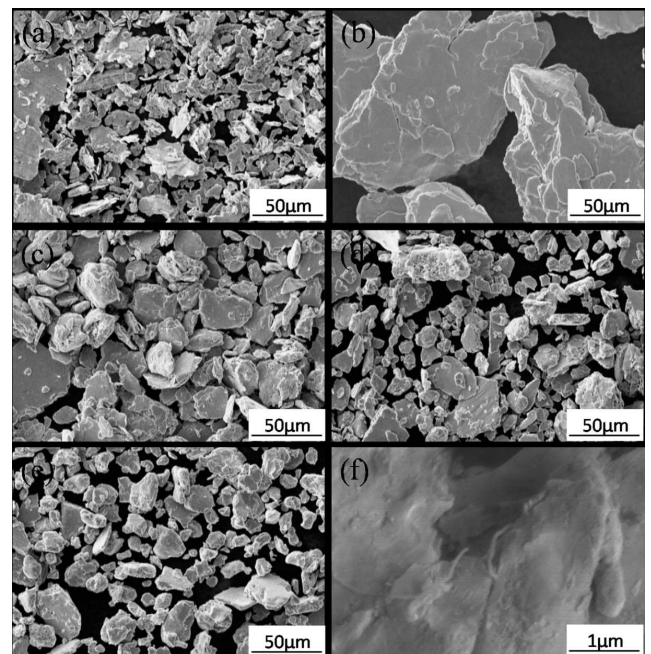


Fig. 2. SEM micrographs showing the morphology of Cu/CNT nanocomposite powder after the milling times of (a) 1 h, (b) 8 h, (c) 16 h, (d) 24 h, (e) 36 h, and (f) CNTs on the surface of particles after mechanical milling for 1 h.

During mechanical milling process, the powders are subjected to high-energy collision, which causes plastic deformation, cold welding and fracture of the powders. Plastic deformation and cold welding are predominant during the initial stage of mechanical milling, in which deformation leads to a change in particle shape, Fig. 2a, and cold welding leads to an increase in particle size and the formation of large layered particles, Fig. 2b. With prolonging mechanical milling, the copper particles become flattened by the impact forces exerted on the powder by the milling medium. During mechanical milling, the CNTs are randomly embedded into the deformed, soft Cu matrix to form coarse Cu/MWCNTs composite powders. The predominant mechanism in this stage is plastic deformation and cold welding. With further milling, the ability of the particles to accept further plastic deformation is diminished. Therefore, fracturing becomes a significant process, which leads to a decrease in particle size, as shown in Fig. 2c. During this stage, the large particles were subjected to continuous fragmentation to form finer particles with a narrower particle size distribution. As welding happens in the process, particle morphology is altered by flattened particle pile-up. Welding and fracture mechanisms then reach equilibrium, promoting the formation of composite particles with randomly orientated interfacial boundaries. The latter stages of the milling process involve particle fracture, and results in further deformation and/or fragmentation of the particles. After 16 h milling, the Cu/MWCNTs composite particles become slightly finer, as seen in Fig. 2d and e. Resistance to the fracture increases with a decrease in fragment size. After 24 h ball milling, the large number of the Cu/MWCNTs composite particles showed a spherical morphology with fewer fine fragments on the particle surfaces (Fig. 2d). Figure 2f shows high magnification micrograph of the Cu/CNTs powder surface after 1 h mechanical milling. Dispersion of CNTs on Cu particles can be seen easily on the surface of the particle. The particle sizes of the composite after mechanical milling for different times are presented in Table I. The table reveals that as the milling time is increased from 8 to 36 h, the D_{50} decreases from 31.53 to 5.90 μm .

TABLE I

The characteristics of the mechanically milled powder for various milling durations.

| Milling time [h] | D_{50}^* [μm] | Grain size [nm] | HV [kgf/cm ²] |
|------------------|------------------------------|-----------------|---------------------------|
| 0** | 31.76 | 3141 | 62.3 \pm 7.3 |
| 1 | 14.95 | 38.8 | 85.4 \pm 10.1 |
| 8 | 31.53 | 18.4 | 117.9 \pm 15.1 |
| 16 | 17.36 | 14.7 | 241.7 \pm 11.1 |
| 24 | 6.29 | 14.6 | 261.4 \pm 12.1 |
| 36 | 5.90 | 12.4 | 265.7 \pm 17.4 |

* D_{50} denotes the particle size at 50 pct of the cumulative curve.

**Properties of Cu particles.

3.2. Microstructure

Results of microstructural investigation on the mechanically milled nanocomposite powder are shown in Fig. 3. As usual, copper matrix grain refinement is clearly indicated by the broadening of width of the Cu diffraction peak at its half maximum intensity. XRD results were analyzed to measure the crystallite size of copper matrix using Williamson–Hall's formula [15].

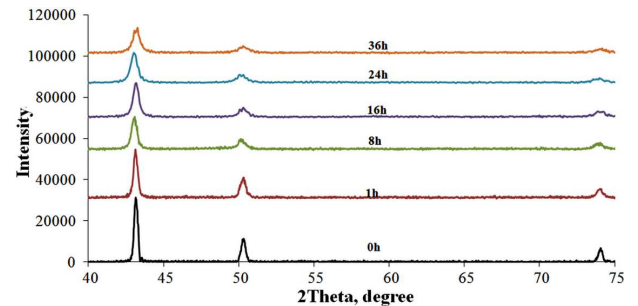


Fig. 3. XRD patterns of mechanically milled powders for various durations.

According to the Williamson–Hall equation and using four planes diffractions, the mean grain sizes of copper in the nanocomposite powder for different mechanical milling times are presented in Table I, which indicates that the crystallite size decreases with increasing milling time, and the average crystallite size is kept at 12.4 nm at the end of the process. The small crystallite size can induce an increase in microhardness of the powder as the values reported in Table I.

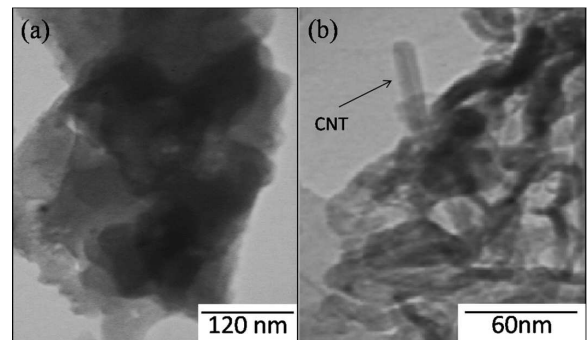


Fig. 4. TEM micrographs of (a) nanograin Cu matrix and (b) CNT implanted into the nanocomposite, after mechanical milling for 8 h.

The microstructure of mechanically milled Cu–CNT nanocomposite consists of CNT embedded within a Cu matrix. TEM micrographs of the Cu/CNT nanocomposite powder after milling time of 24 h is shown in Fig. 4. Figure 4a shows a typical microstructure of copper matrix, which is characterized by a very fine nanocrystalline structure. The grain size obtained from TEM micrographs (24 nm) is slightly larger than the value determined by XRD results. Figure 4b shows a TEM micrograph of the nanocomposite with a CNT embedded in Cu matrix.

3.3. Compressibility

Figure 5 shows the variation of green density of the Cu-CNT powder mechanically milled for various times as a function of applied pressure. In general, the curves indicate the typical powder compressibility behavior for metallic powders, i.e. the density increases with increasing the compaction pressure with a decelerating rate at higher pressures. The compaction of powders is divided

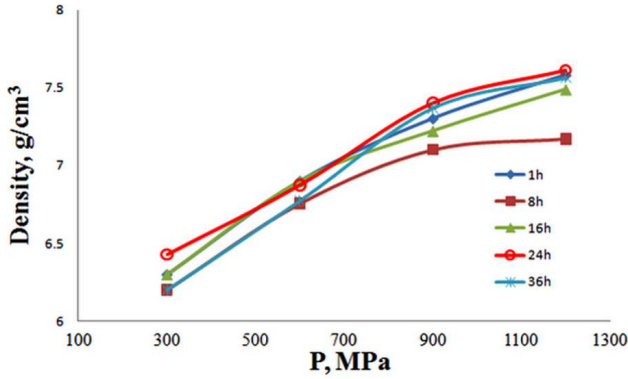


Fig. 5. Effect of pressure on green density of mechanically milled powders.

into stages and each stage is considered to be interrelated in terms of the physical and mechanical properties of powder particles [16]. The initial stage of compaction involves particle rearrangement; this stage is largely affected by particle size and shape. In the second stage, it is considered that elastic and plastic deformation took place and that the mechanical properties are dominant. The final stage is considered to be almost entirely due to cold working of the bulk material and is affected by deformation and work hardening of particles. However, due to differences in density and stress distributions there is likely to be an overlap of the different stages during the consolidation process. It can be seen that the large flaky particles have the lowest green density and semispherical particles have the highest green density during compression. Shape, size distribution, and hardness of the particles can affect the forces appearing in the contact points of the particles and deformation behavior of the particles during compression. The 1 h mechanically milled powder is ductile and flaky, so possesses good compressibility at higher pressures. At mechanical milling for 8 h, the powder is work hardened, large and has flaky shape; therefore it poses the lowest density at all pressures. With prolonging the mechanical milling time up to 8 h, the hardness increases, and the ratio of flaky to spherical particles decreases due to fracturing mechanism. After 16 h mechanical milling, the powder experiences a little change in hardness but a decrease in particle size. It seems that the particles can rearrange easily under applied load and fill the void during compaction at this stage. For 36 h mechanical milling, the powder has the highest hardness and ratio of spherical to flaky particles with small size; therefore densification rate of the milled powder at low and moderate pressures is lower.

The powder plastic deformation capacity during the cold uniaxial compaction process was estimated using three different statistical models of the Akbarpour et al. [16], Heckel [17] and Ge [19] which are given in Table II, where D and P are the fractional density and applied pressure, respectively. K and B are fitting parameters.

TABLE II

The used analytical models.

| | |
|----------------------------|---|
| Heckel Eq. [17] | $\ln\left(\frac{1}{1-D}\right) = KP + B$ |
| Panelli and Filho Eq. [18] | $\ln\left(\frac{1}{1-D}\right) = KP^{1/2} + B$ |
| Ge Eq. [19] | $\log\left(\ln\left(\frac{1}{1-D}\right)\right) = K \log P + B$ |

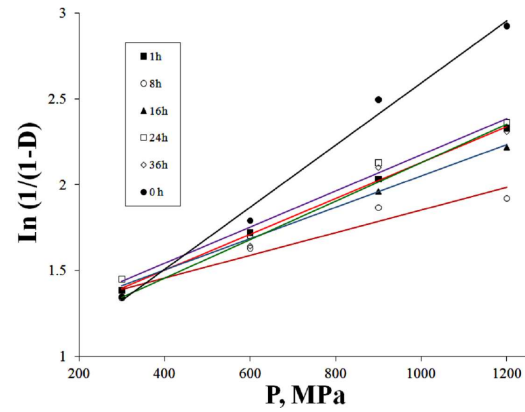


Fig. 6. Experimental data of Cu-CNT nanocomposite powder fitted by Heckel equation.

Figure 6 shows the fitting graphs by using Heckel [17] equation, and Table III summarizes K and σ_y values for different mechanical milling times. K is an indicator of the plastic deformation capability of the particles and is directly related to the yield stress of the compacts (σ_y), e.g., $K = 1/3\sigma_y$ for Heckel equation [17].

TABLE III

The fitting parameter (K) and yield strength obtained from statistical analysis of the experimental data. The values in the parentheses are the regression coefficients (R^2).

| MM [h] | Heckel Eq. [$\times 10^{-1}$ MPa] | Panelli-Filho Eq. [MPa $^{-0.5}$] | Ge Eq. [MPa $^{-1}$] | σ_y [MPa] |
|--------|------------------------------------|------------------------------------|-----------------------|------------------|
| 0 | 0.0018(0.990) | 0.093(0.979) | 0.568(0.977) | 185 |
| 1 | 0.0010(0.999) | 0.054(0.995) | 0.369(0.991) | 333 |
| 8 | 0.0007(0.970) | 0.035(0.968) | 0.271(0.984) | 476 |
| 16 | 0.0009(0.994) | 0.047(0.998) | 0.334(0.996) | 370 |
| 24 | 0.0011(0.997) | 0.054(0.977) | 0.359(0.966) | 303 |
| 36 | 0.0011(0.982) | 0.058(0.981) | 0.403(0.976) | 303 |

According to Table III, the mechanically milled Cu-CNT powders show better consistency with the Heckel equation during uniaxial compression. In general, with increasing mechanical milling time/grain refinement, the yield strength enhances continually while in the yield

strength calculated by Heckel equation, the values at higher mechanical milling times are showing a decrease, which maybe is the effect of particle shape or load transferring between particles on this parameter.

3.4. Densification

Figure 7a (curve 1) shows sintered density of the Cu–CNT samples mechanically milled for 24 h sintered at different temperatures for 1 h in a vacuum furnace. It can be seen that sintered density of the Cu–CNT materials depends greatly on temperature. As sintering temperature rises, linear sintering shrinkage of the Cu–CNT compacts and densities of the composite increase. When Cu–CNT compacts were sintered at 900 °C, the sample had a relative density near 91%. Figure 7b (curve 2) shows sintered density of the Cu–CNT samples mechanically milled for different times sintered at the temperature of 900 °C for 1 h. The powder mechanically milled for 1 h showed the highest relative density as a result of partially work hardened microstructure and higher green density. The sintered powders showed densification behavior similar to green density with increasing mechanical milling time which illustrates the important role of powders morphology and hardness on densification of mechanically milled Cu–CNT powders. Figure 7b shows the microstructure of sintered nanocomposite mechanical milled for 24 h at temperature of 900 °C after etching. The figure shows the microstructure including ultrafine grains even after sintering at a high temperature.

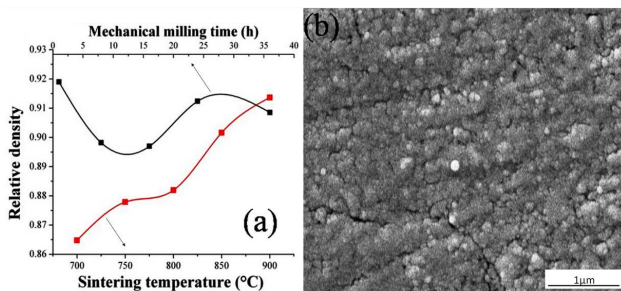


Fig. 7. (a) Effects of sintering temperature and mechanical milling duration on density of the nanocomposite, and (b) SEM micrograph showing the etched microstructure of sintered nanocomposite (mechanical milling time 24 h, $T = 900$ °C and sintering time of 1 h).

4. Conclusions

Cu/CNT nanocomposite powders were produced via high energy mechanical milling. The morphology, microstructure and microhardness of the powders during the fabrication process were evaluated. The powders were subjected to uniaxial compression, and the effect of powders properties on green density studied. Three analytical models were used to estimate the compressibility behavior of mechanically milled powders and were compared with the experimental values. Finally, the green compacts with different mechanical milling times were vacuum sintered. The conclusions are as follows:

1. Cu/CNT nanocomposite powder with nanosized grains can be fabricated by the mechanical milling of the elemental materials. During mechanical milling, CNTs were implanted in Cu.
2. The nanocomposite powder showed better consistency with the Heckel equation during uniaxial compression.
3. The addition of CNTs accelerated the morphological and microstructural evolution during mechanical milling, and influenced the compressibility by alteration of the powder morphology and size.
4. The vacuum sintered samples showed densification behavior identical to green compact with increasing mechanical milling time. The nanocomposite reached to the maximum relative density of $\approx 91\%$ at the optimum sintering temperature.

References

- [1] P. Calvert, *Nature* **399**, 210 (1999).
- [2] E.T. Thostenson, Z.F. Ren, T.W. Chou, *Compos. Sci. Technol.* **61**, 1899 (2001).
- [3] J.P. Salvetat, J.M. Bonard, N.H. Thomson, A.J. Kulik, L. Forro, W. Benoit, L. Zuppiroli, *Appl. Phys. A* **69**, 255 (1999).
- [4] M.R. Akbarpour, E. Salahi, F. Alikhani Hesari, A. Simchi, H.S. Kim, *Mater. Sci. Eng. A* **572**, 83 (2013).
- [5] A. Maqbool, M.A. Hussain, F.A. Khalid, N. Bakhsh, A. Hussain, M.H. Kim, *Mater. Charact.* **86**, 39 (2013).
- [6] N. Nayan, S.V.S.N. Murty, S.C. Sharma, K.S. Kumar, P.P. Sinha, *Mater. Charact.* **62**, 1087 (2011).
- [7] S.E. Shin, D.H. Bae, *Mater. Charact.* **83**, 170 (2013).
- [8] E. Yoon, D. Lee, B. Park, M.R. Akbarpour, M. Farvizi, H. Kim, *Met. Mater. Int.* **19**, 927 (2013).
- [9] S.R. Dong, J.P. Tu, X.B. Zhang, *Mater. Sci. Eng. A* **313**, 83 (2001).
- [10] S.R. Bakshi, D. Lahiri, A. Agarwal, *Intl. Mater. Rev.* **55**, 41 (2010).
- [11] B.J. Kim, S.Y. Oh, H.S. Yun, J.H. Ki, C.J. Kim, S. Baik, B.S. Lim, *J. Nanosci. Nanotechnol.* **9**, 7393 (2009).
- [12] K.T. Kim, S.I. Cha, S.H. Hong, S.H. Hong, *Mater. Sci. Eng. A* **430**, 27 (2006).
- [13] A.K. Shukla, N. Nayan, S.V.S.N. Murty, K. Mondal, S.C. Sharma, K.M. George, S.R. Bakshi, *Mater. Charact.* **84**, 58 (2013).
- [14] S.J. Yoo, S.H. Han, W.J. Kim, *Carbon* **61**, 487 (2013).
- [15] G.K. Williamson, W.H. Hall, *Acta Metall.* **1**, 22 (1953).
- [16] M.R. Akbarpour, E. Salahi, F. Alikhani Hesari, A. Simchi, H.S. Kim, *Ceram. Int.* **40**, 951 (2014).
- [17] R.W. Heckel, *Trans. Metall. Soc. AIME* **221**, 671 (1961).
- [18] R. Panelli, F.A. Filho, *Powder Technology* **114**, 255 (2001).
- [19] R. Ge, *Int. J. Powder. Metall.* **27**, 211 (1991).